



Published in final edited form as:

Pharmacol Res. 2010 May ; 61(5): 385–390. doi:10.1016/j.phrs.2010.01.007.

## Diet-Induced Obesity Alters Vincristine Pharmacokinetics in Blood and Tissues of Mice

James W. Behan<sup>a</sup>, Vassilios I. Avramis<sup>b,c,d</sup>, Jason P. Yun<sup>a</sup>, Stan G. Louie<sup>e</sup>, and Steven D. Mittelman<sup>a,c,d</sup>

<sup>a</sup> Division of Endocrinology, Diabetes & Metabolism (JWB, JPY, SDM), Childrens Hospital Los Angeles, 4650 Sunset Blvd., Los Angeles, CA 90027, USA

<sup>b</sup> Division of Hematology & Oncology (VIA), Childrens Hospital Los Angeles, 4650 Sunset Blvd., Los Angeles, CA 90027, USA

<sup>c</sup> Saban Research Institute (VIA, SDM), Childrens Hospital Los Angeles, 4650 Sunset Blvd., Los Angeles, CA 90027, USA

<sup>d</sup> Department of Pediatrics (VIA, SDM) and Norris Cancer Center (VIA, SDM), Keck School of Medicine, University of Southern California, Los Angeles, CA, 90033, USA

<sup>e</sup> School of Pharmacy (SGL), University of Southern California 1985 Zonal Avenue, Los Angeles, CA 90033, USA

### Abstract

Obesity is associated with poorer outcome from many cancers, including leukemia. One possible contributor to this could be suboptimal chemotherapy dosing in obese patients. We have previously found that vincristine (VCR) is less effective in obese compared to non-obese mice with leukemia, despite weight-based dosing. In the present study, we administered <sup>3</sup>H-VCR to obese and control mice to determine whether obesity would cause suboptimal VCR exposure. Blood VCR concentrations were fitted with a 3-compartment model using pharmacokinetic analysis (two-stage PK) in 3 subsets of VCR concentrations vs. time method. Tissue and blood VCR concentrations were also analyzed using non-compartmental modeling. Blood VCR concentrations showed a triexponential decay and tended to be slightly higher in the obese mice at all time-points. However, the  $t_{1/2\beta}$  and  $t_{1/2\gamma}$  were shorter in the obese mice (9.7 vs. 44.5 minutes and 60.3 vs. 85.6 hours, respectively), resulting in a lower  $AUC_{0\rightarrow\infty}$  (13,099 vs. 15,384 ng/ml\*hr). Had the dose of VCR been “capped”, as is done in clinical practice, the  $AUC_{0\rightarrow\infty}$  would have been 36% lower in the obese mice than the controls. Tissue disposition of VCR revealed a biexponential decay from spleen, liver, and adipose. Interestingly, VCR slowly accumulated in the bone marrow of control mice, but had a slow decay from the marrow in the obese mice. Thus, obesity alters VCR PK, causing a lower overall exposure in circulation and bone marrow. Given the high prevalence of obesity, additional PK studies should be performed in obese subjects to optimize chemotherapy dosing regimens.

---

Corresponding Author and Reprint Requests: Steven D. Mittelman, MD, PhD, Childrens Hospital Los Angeles, Division of Endocrinology, MS, #61, 4650 Sunset Boulevard, Los Angeles, CA 90027, Phone: 1 (323) 361-7653, Fax: 1 (323) 906-8013, smittelman@chla.usc.edu.

**Publisher's Disclaimer:** This is a PDF file of an unedited manuscript that has been accepted for publication. As a service to our customers we are providing this early version of the manuscript. The manuscript will undergo copyediting, typesetting, and review of the resulting proof before it is published in its final citable form. Please note that during the production process errors may be discovered which could affect the content, and all legal disclaimers that apply to the journal pertain.

## Keywords

Obesity; leukemia; chemotherapy; vincristine; pharmacokinetics

---

## 1. Introduction

There is growing evidence that obesity is associated with increased mortality from cancer, including leukemia [1–4]. Increased leukemia mortality may be attributed in part to an increase in incidence in obese individuals [5,6]. However, patients who are obese at the time they are diagnosed with acute lymphoblastic leukemia or acute myeloid leukemia have significantly higher mortality than their normal weight counterparts [7–9]. There are a myriad of possible explanations for this, including delayed diagnosis, more aggressive cancer, poor compliance, and impaired immunity. It is also conceivable that dosing practices of chemotherapies, such as *a priori* dose reduction and dose capping may contribute to suboptimal levels in obese patients [10–12]. Obesity is a complex state associated not only with an increase in total body size, but also increased fat distribution, relative decrease in lean body mass [13], and altered cardiac [14], liver [15], and renal function [16,17]. Despite the importance of accurate chemotherapy dosing, and the increasing prevalence of obesity, few pharmacokinetic studies have been performed to elucidate the clinical impacts of obesity on chemotherapeutic agents pharmacokinetics and ultimate long term survival [18].

Vincristine (VCR), a potent antimicrotubule agent, is a seminal drug in the treatment of multiple cancers, including hematological malignancies, in children and adults [19,20]. The sensitivity of leukemia cells to VCR has been demonstrated to correlate with event-free survival [21,22]. We recently reported that obese mice transplanted with syngeneic leukemia cells exhibited impaired survival after VCR treatment when compared to control mice [23]. In that study, we had dosed VCR in proportion to body weight, and thus effectively matched the blood and tissue VCR concentrations in the obese and control mice. However, clinical dosing of VCR in pediatric cancer patients is proportional to body surface area, and is generally “capped” at 1 square meter. Thus, an obese 18 year old generally receives approximately the same total VCR dose as an average 8–9 year old.

Recently, there have been many studies examining the pharmacokinetics of VCR in young children and adolescent ALL patients [24–27]. Some of these attempted to link the observed differences in the variable response (outcomes) post-combination regimens to VCR exposure. Based on detailed PK analyses, one study concluded that there is no pharmacokinetic rationale to “limit” the dose in adolescent ALL patients [25]. Although it is clear that variability in expression and polymorphisms of the CYP3A isoforms of the P450 metabolic complex system could account for some of the variability observed in VCR PK [28–30], it is likely that other factors, such as obesity and concomitantly administered medications, may also play a role in VCR exposure in patients.

Given that obese patients with leukemia and other cancers have poorer outcomes, and receive less VCR per kg body weight than lean patients, the present study was designed to elucidate whether diet-induced obesity alters the blood and tissue pharmacokinetics of VCR in mice.

## 2. Methods

### 2.1. Mouse Model

C57Bl/6J mice were purchased from Jackson Laboratories (Bar Harbor, ME). Male mice were weaned at 4 weeks of age and fed a high fat diet (60% of calories from fat, Research Diets D12492, New Brunswick, NJ) or a control diet (10% of calories from fat, D12450), and used

for experiments at 17 weeks of age. All animal experiments were approved by the Childrens Hospital Los Angeles Institutional Animal Care and Use Committee, and performed in accordance with the U.S. Public Health Service Policy on Humane Care and Use of Laboratory Animals.

## 2.2 VCR Pharmacokinetics Experiment

Twenty obese and 21 control mice received tail-vein injections of tritiated vincristine ( $[^3\text{H}]$  VCR) proportional to body weight (specific activity 75  $\mu\text{Ci}/\text{mg}$ ; dose 0.5  $\text{mg}/\text{kg}$ , American Radiolabeled Chemicals, Inc., St. Louis, MO). The VCR was synthesized by tritium gas catalyzed exchange, and therefore the molecule was uniformly labeled in random positions. Blood samples were collected from a subset of animals ( $n=8$  per group) from the submandibular venous plexus at  $t=5$  minutes using GoldenRod lancets (Medipoint, Inc., Mineola, NY) into EDTA coated tubes. Mice were sacrificed in groups of 3 to 5 at  $t=0.25, 0.5, 1, 3, 8,$  and 24 hours post-injection.

## 2.3 VCR Measurements

Whole blood and tissue specimens were rapidly removed, and then solubilized using Solvable (Perkin Elmer, Waltham, MA). The brown fat depot was removed from the intrascapular space and identified by its tan color. Whole blood, spleen, and liver were decolorized using 30%  $\text{H}_2\text{O}_2$ . Samples were then read on a scintillation counter (TriCarb 2100TR, Perkin Elmer) using ReadySafe (Beckman Coulter, Inc., Fullerton, CA). Recovery was determined by spiking tissues (blood, spleen, and liver) from an un-injected mouse with a known quantity of  $^3\text{H}$ -vincristine and processing in parallel with experimental samples.

Additional plasma samples from the 24 hour time-point were used to validate the tritium assay by comparing the concentration using an LC/MS assay [31]. The evaporated samples from cellular extracts or media were then reconstituted in 50  $\mu\text{L}$  of running buffer consisting of 45% methanol and 55% of 0.1% formic acid (v/v). The entire solution was vortexed for 1 minute and then centrifuged at 13,000 rpm at  $4^\circ\text{C}$  for 10 minutes. Afterward, the clarified supernatant was transferred into an injection vial, where 25  $\mu\text{L}$  of the sample were injected into an Agilent 1100 HPLC system linked onto an API 3000 (Applied Biosystems, Foster City, CA). The analytes were separated using a C18 ACE column with the following dimensions  $50 \times 3.0$  mm. The analytes were eluted using mobile phase consisting of 45% methanol and 55% of 0.1% formic acid (v/v), where the flow rate was set at 350  $\text{cc}/\text{min}$ . The amount of VCR was determined using API 3000, where the  $m/z$  to transition ion was monitored  $413.6 \rightarrow 392.4$  and  $406.5 \rightarrow 272.0$  for vincristine and vinblastine, respectively. Using this method, we have previously measured VCR with the lowest level of quantification of 0.02 nM. The standard curve for the assay had an  $r^2 = 0.998$ .

## 2.4 Pharmacokinetic (PK) -analytical modeling

Total blood VCR levels were analyzed by the two-stage PK populations method using NONLIN software [32]. The data were fit to a 3-compartment open pharmacokinetic model. Specifically, the equation used for the VCR concentration-time fit in blood is shown in equation 1:

$$C(t) = A \cdot e^{-\alpha t} + B \cdot e^{-\beta t} + C \cdot e^{-\gamma t} \quad 1$$

Compartmental modeling was also used to accommodate tissue VCR concentrations. It was apparent that the tissues tested achieved immediate equilibrium, i.e. within 15 minutes. The only exception was the bone marrow. Hence, the equation describing the fate of VCR after the first 15 minutes in spleen, liver, fat, and brown fat is:

$$C(t)_{\text{tissue}} = B \cdot e^{-\beta t} + C \cdot e^{-\gamma t} \quad 2$$

For bone marrow, the VCR concentration showed an initial accumulation phase in both groups, but a slower decay in the obese mice, and a slow accumulation in the lean mice. Thus, the equations describing bone marrow concentrations were:

$$\begin{aligned} C(t)_{\text{obese-marrow}} \\ = B \cdot e^{+\beta t} \\ + C \cdot e^{-\gamma t}, \text{ and} \end{aligned} \quad 3a$$

$$\begin{aligned} C(t)_{\text{nonobese-marrow}} \\ = B \cdot e^{+\beta t} \\ + C \cdot e^{+\gamma t}, \text{ for the lean mice.} \end{aligned} \quad 3b$$

Initial estimates from this compartmental model were then used to derive a non-compartmental analysis using customized subroutines based on the methods previously described [32,33]. Using these methods, blood VCR clearance was estimated by the equation:

$$\begin{aligned} \text{Total body clearance (CL}_T) \\ = \text{Dose} / \text{AUC}_{0 \rightarrow \infty} \end{aligned} \quad 4$$

The apparent volume of the central compartment of distribution (V<sub>dc</sub>) and apparent volume of distribution at steady-state (V<sub>dss</sub>) were respectively calculated by the following equations:

$$V_{dc} = \text{Dose} / (A + B + C), \text{ and} \quad 5$$

$$\begin{aligned} V_{dss} = \text{Dose} [ (A/\alpha^2) + (B/\beta^2) + (C/\gamma^2) ] \\ / (\text{AUC}_{0 \rightarrow \infty})^2 \end{aligned} \quad 6$$

Finally, a limited physiological pharmacokinetic model was derived from the blood and tissue compartmental modeling parameters.

The averages per time-point VCR concentrations were analyzed by a NONMEM 3-compartment open model subroutine. The solutions were super-imposable to the 2-stage compartmental method described above, thus validating our solution. Moreover, randomly assigned animal time-points were assigned as individual observations of VCR pharmacokinetics. These multiple sets of PK profiles were attempted to be analyzed by NONMEM; however, due to the high variance in this group of mice, the program did not converge.

## 2.5 Calculations

Tissue specific activity (SA) was calculated from the raw cpm data divided by the counter efficiency, and our determined processing recovery. Tissue SA was divided by stock solution

SA to derive tissue VCR concentrations. Blood and tissue VCR levels at each timepoint were compared between groups with t-tests. Percentage of the injected dose was log-transformed prior to comparison by t-test due to non-normal distribution. All the data are expressed as mean  $\pm$ S.D.

### 3. Results

Mice raised on the high fat diet were significantly heavier than control mice ( $40.3 \pm 1.6$  vs.  $29.8 \pm 1.8$  g,  $p < 0.0001$ ), and since VCR was dosed proportional to body weight, obese mice received ~28% more VCR per injection than controls. The VCR injections were well tolerated by all animals, as determined by observation of behavior. At all time-points, blood vincristine concentrations were higher in the obese mice than the controls and followed a tri-phasic decay (Figure 1). Tissue levels of VCR were comparable between obese and nonobese mice in spleen, liver, brown fat, and bone marrow, while they tended to be slightly higher in the white adipose depots in the obese mice (Figure 1). By 3 hours after the injection,  $0.10 \pm 0.01\%$  of the injected VCR could be accounted for in the white adipose tissue of the control mice, while  $0.39 \pm 0.14\%$  was in the white adipose tissue of obese mice ( $p = 0.025$ , Figure 2). This proportion remained relatively constant in the control mice, while it tended to increase in the obese mice, so that at 24 hours,  $0.08 \pm 0.03\%$  of the injected dose could be accounted for in the white adipose tissue of the non-obese mice, compared to  $0.66 \pm 0.43\%$  of the dose in the obese mice ( $p = 0.062$ ).

#### 3.1 Compartmental Model

No samples were excluded from the analysis. The final pharmacokinetic model was a linear, three-compartment-open model that described the VCR kinetics in blood, with the tissues achieving rapid equilibrium (15 min) except for the marrow in the lean group of mice. From this, a linear, two-compartment model was used that described the VCR in tissues (spleen, liver, fat, brown fat and marrow, Fig. 3). These analyses showed that a triexponential PK model fitted our blood data better than a biexponential in both groups of mice with VCR concentrations over time (F-test). The estimates of the PK parameters are summarized in Tables 1 and 2. The fitted peak blood VCR concentration was much higher in the obese than the non-obese mice. However, all three half-lives describing the decay were shorter in the obese vs. the non-obese mice. These differences resulted in an ~17% higher  $AUC_{0-24}$  in obese mice, while the projected total exposure ( $AUC_{0-\infty}$ ) was ~15% lower in the obese mice. These AUC changes occurred despite the significantly higher total dose of VCR administered to the obese mice.

The only difference in VCR kinetics from the tissues in the two groups is that in the non-obese mice, the VCR accumulated in a classical Michaelis-Menten kinetics uptake in the bone marrow environment for the duration of the experimental measurements, as if the drug was binding to a protein pool, without any apparent elimination (Figure 3). In contrast, in the obese mice, VCR accumulated in the bone marrow well up to the 8 hours (second distribution phase) but then it was eliminated with an apparent mono-exponential decay either via the classical route or directly in the central compartment (Figure 3, dotted arrow).

#### 3.2. Noncompartmental PK analyses Model

Using initial estimates derived from the compartmental model, we derived a noncompartmental analysis using previously described subroutines. The  $V_{DSS}$  was slightly lower in the obese mice (3.16 vs. 3.81 ml/g), though they were similar when expressed per mouse rather than per gram (114 vs. 127 ml/mouse), signifying possibly a higher body storage of VCR in the obese mice. However, the total body clearance ( $CL_T$ ) was slightly higher in the obese mice than the lean (0.038 vs. 0.033 ml/hr). These results corroborate the fitted higher peak blood VCR concentration and lower  $AUC_{0-\infty}$  in the obese mice from the compartmental model.

### 3.3 LC/MS results

The VCR concentrations measured by LC-MS on the 24 hour plasma samples showed no difference between obese and control mice ( $69 \pm 10$  vs.  $70 \pm 10$  ng/mL,  $p = n.s.$ ) These values were ~70% of the values obtained from the tritium reading, likely reflecting tritium signal from VCR metabolites, differences between plasma and whole blood, and different methodologies.

## Discussion

Detailed PK evaluations have demonstrated the high variability of VCR PK between individuals [26]. Despite this variability, there is some evidence that VCR kinetics is related to treatment outcome for diseases such as standard-risk ALL [24]. In the present study, we have investigated the effect of diet-induced obesity in mice on the pharmacokinetics of a single intravenous bolus of  $^3\text{H}$ -VCR. The blood VCR profiles in both groups of mice were best fit by a tri-exponential decay, with a fast redistribution phase ( $t_{1/2,\alpha} = 3\text{--}4$  minutes), during which the VCR is presumably moving from the blood to other tissue compartments, and two slower decays. This is similar to blood and plasma profiles observed in other studies, where vincristine levels have been generally described as either bi- or tri-exponential curves in rodents [34–36], dogs [34], and humans [25,26,37–40]. These profiles were used to derive a linear 3-compartment open model.

Using these models, we found that obese mice exhibited smaller volumes of distribution (per gram body weight), along with shorter terminal half-lives of elimination. The shorter half-lives may have been due to more rapid metabolism, or may reflect more extensive distribution to a remote compartment, such as adipose tissue. Although CYP 3A4 activity, which is primarily responsible for VCR metabolism, was not quantified in this study, severe obesity induced by leptin knockout in the same mouse strain had no effect on CYP 3A4 expression or protein level [41]. In any case, the shorter half-lives were associated with lower overall exposure ( $\text{AUC}_{0 \rightarrow \infty}$ ) to VCR. To the extent that the anti-leukemic activity of VCR depends on the length of time it remains over some therapeutic threshold concentration [42], this increase in clearance (CLT) could impair the effectiveness of this drug, especially after multiple doses in patients.

Chemotherapy dosing in pediatric patients is generally based on body surface area, but extensive pharmacokinetic and pharmacodynamic studies in obesity have not been performed, and thus the optimal dosing regimens in these patients have not been delineated. In fact, some chemotherapeutic drugs, such as VCR, are lipophilic, and thus may accumulate in adipose tissue, which is more abundant in overweight patients. Since body weight and particularly fat mass are disproportionately increased relative to surface area in obese patients, chemotherapy concentrations may be suboptimal in these patients. Furthermore, VCR dosing is generally “capped” to avoid neurotoxicity. With this cap of 2 mg per dose, an obese adolescent will receive the same dose of VCR as a child of  $1 \text{ m}^2$ , or an average 8 year old. Therefore, it is possible that current dosing practices will lead to lower tumor exposure to VCR and other chemotherapies in older, heavier children. A recent study concluded that in adolescent ALL patients there is no pharmacokinetic rationale to “limit” the dose [25]. If there is significant distribution of these drugs in adipose tissue, this could further exacerbate the problem.

The risks of under- or over-dosing obese patients with chemotherapeutic agents has been highlighted by multiple case reports and studies in the literature (reviewed in [12]). However, there is little consensus as to the optimal dosing strategies to use in obese patients. Part of the difficulty comes from the inherent variability observed in the PK of chemotherapeutic drugs [12]. In addition, limited understanding of the relationships between the pharmacokinetic/ pharmacodynamics and efficacies of chemotherapies make these decisions more arbitrary. The limited data that do exist suggest that adjustment of actual body weight or capping of chemotherapy doses may be detrimental to outcomes [10–12]; however, prospective PK studies

in obese patients are yet to be performed. In the present study, we attempted to further expand our understanding of the PK of VCR in obesity—not only in the blood, but also its disposition and elimination kinetics from important metabolic organs and leukemia microenvironments (e.g. spleen, bone marrow, etc.). Our findings may provide further evidence for rational design of clinical studies to evaluate the PK of VCR in obese patients.

The clinical importance of VCR PK was demonstrated in an elegant manner by Lönnerholm et al., who analyzed the PK of the first dose of VCR in children with newly diagnosed leukemia [24]. These authors found that standard risk leukemia patients with a VCR AUC less than the median had a relative risk of relapse of 5.8 compared to those with an AUC greater than the median. Although the subjects in these studies were mostly not obese (Lönnerholm, personal communication), these data suggest that if obesity was to decrease VCR exposure, this could contribute to a poorer prognosis in these patients. Indeed, since VCR clearance does not change with VCR dose [38], we can estimate that if the obese mice had been dosed with the same total amount of VCR as the non-obese mice, (i.e. if we had “capped” their doses), their  $AUC_{0-24}$  and  $AUC_{0-\infty}$  would have been 13% and 36% lower than the non-obese mice, respectively.

One weakness in the present study is that we were unable to evaluate protein bound vs. free VCR. It is possible that albumin and protein levels could have been altered in the obese mice, though it has been shown that mice made obese by a moderately high fat diet (45% of calories from fat) have similar rates of albumin synthesis as control mice [43]. Also, though albumin has a clear effect on VCR action *in vitro* [44], the clinical relevance of protein binding alterations in protein binding of drugs *in vivo* is questionable [45].

The measurement of VCR using tritium activity may include VCR metabolites along with the parent compound. Thus, any differences in metabolism between the groups (or in different tissues) could increase the errors introduced by the model assumption that tritium signal reflects VCR concentration. However, our LC/MS measure on the 24 hour sample confirms that the tritium signal in the blood was primarily from the parent drug, and any errors introduced by including the metabolites would not likely be very different between the two groups of mice. Also, some VCR metabolites might maintain their antitumor activity, perhaps allowing this “grouping”.

Another limitation of this study is the short sampling schedule, which ended at 24 hours. This was done for logistical reasons along with the high cost of this obese mouse model. Since the terminal half-lives were considerably longer than 24 hours, this sampling may have led to errors in the estimation of the terminal half-life, and therefore of the  $AUC_{0-\infty}$  and TCL. However, even modest errors in this parameter would not change our primary conclusion that obesity can decrease VCR exposure after an intravenous dose in obese mice, particularly if this dose is adjusted or capped.

A major strength of this study is that we used multiple PK modeling methods to derive and validate robust final PK model parameters for VCR in the obese and non-obese mice. In addition, VCR concentration was also analyzed in relevant tissues, which confirmed that tissue VCR distribution was well-matched when the drug was administered proportionally to body weight. These tissue VCR concentrations allowed us to derive a limited physiological model, and to evaluate tissue VCR kinetics, which may be important for interpreting future PK studies in lean and obese patients.

In summary, in the present study despite its limitations, we have developed an appropriate compartmental PK model for VCR, accommodating many mammalian tissues, using a limited physiological model (Figure 3). In addition, these PK estimations have been validated using non-compartmental analyses. Using this 3-compartment open PK model, we demonstrated that current dosing practices with VCR, particularly “capping”, are likely to lead to under-dosing

of this important anticancer drug, and decreased VCR exposure in obese patients. However, definitive studies in obese and lean human subjects will be necessary to test for this effect. This first step will facilitate the use of novel study designs in obese and non-obese oncology patients, utilizing limited/sparse PK drug sampling strategies, along with the development of a validated limited-pharmacokinetic physiological model for this drug. Given the increasing prevalence of obesity world-wide, as well as evidence that obesity increases cancer incidence and mortality [1], investigating how to optimally treat obese cancer patients is of paramount importance.

## Acknowledgments

The authors would like to thank Eugene Park for assistance with tail-vein injections; Nick Mordwinkin, for performing VCR LC/MS measures, and Donna Foster, for her excellent animal care.

### Funding

The present work was supported in part by grants to S.D.M. from the NIH (National Institute of Child Health and Development K12 Award) and National Cancer Institute (CA139060 and Centers for Transdisciplinary Research on Energetics and Cancer U54 CA 116848), and to S.G.L. from NIH 5 P30 CA 14089-27. The sponsoring agencies had no role in the design or execution of the study or decision to submit the manuscript.

## Nonstandard Abbreviations

AUC	area under-the-curve
HPLC	high-pressure liquid chromatography
LC/MS	liquid chromatograph/mass spectrometry
PK	pharmacokinetics
SA	specific activity
VCR	vincristine

## Reference List

1. Calle EE, Rodriguez C, Walker-Thurmond K, Thun MJ. Overweight, obesity, and mortality from cancer in a prospectively studied cohort of U.S. adults. *N Engl J Med* 2003;348:1625–38. [PubMed: 12711737]
2. Guh DP, Zhang W, Bansback N, Amarsi Z, Birmingham CL, Anis AH. The incidence of co-morbidities related to obesity and overweight: a systematic review and meta-analysis. *BMC Public Health* 2009;9:88. [PubMed: 19320986]
3. Pan SY, DesMeules M. Energy intake, physical activity, energy balance, and cancer: epidemiologic evidence. *Methods Mol Biol* 2009;472:191–215. [PubMed: 19107434]
4. Reeves GK, Pirie K, Beral V, Green J, Spencer E, Bull D. Cancer incidence and mortality in relation to body mass index in the Million Women Study: cohort study. *BMJ* 2007;335:1134. [PubMed: 17986716]
5. Kasim K, Levallois P, Abdous B, Auger P, Johnson KC. Lifestyle factors and the risk of adult leukemia in Canada. *Cancer Causes Control* 2005;16:489–500. [PubMed: 15986104]
6. Larsson SC, Wolk A. Overweight and obesity and incidence of leukemia: a meta-analysis of cohort studies. *Int J Cancer* 2008;122:1418–21. [PubMed: 18027857]
7. Butturini AM, Dorey FJ, Lange BJ, Henry DW, Gaynon PS, Fu C, et al. Obesity and outcome in pediatric acute lymphoblastic leukemia. *J Clin Oncol* 2007;25:2063–9. [PubMed: 17513811]
8. Butturini A, Vignetti M, Gubbiotti S, Meloni G, Recchia M, Di Raimondo F, et al. Obesity Independently Predicts Event Free Survival (EFS) in Adults with BCR-ABL-Negative Acute Lymphoblastic Leukemia (ALL). A Retrospective Analysis of Two GIMEMA Studies. *ASH Annual Meeting Abstracts* 2005;106:1828.



9. Lange BJ, Gerbing RB, Feusner J, Skolnik J, Sacks N, Smith FO, et al. Mortality in overweight and underweight children with acute myeloid leukemia. *JAMA* 2005;293:203–11. [PubMed: 15644547]
10. Sparreboom A, Wolff AC, Mathijssen RH, Chatelut E, Rowinsky EK, Verweij J, et al. Evaluation of alternate size descriptors for dose calculation of anticancer drugs in the obese. *J Clin Oncol* 2007;25:4707–13. [PubMed: 17947717]
11. Georgiadis MS, Steinberg SM, Hankins LA, Ihde DC, Johnson BE. Obesity and Therapy-Related Toxicity in Patients Treated for Small-Cell Lung Cancer. *JNCI Journal of the National Cancer Institute* 1995;87:361–6.
12. Hunter RJ, Navo MA, Thaker PH, Bodurka DC, Wolf JK, Smith JA. Dosing chemotherapy in obese patients: Actual versus assigned body surface area (BSA). *Cancer Treatment Reviews* 2009;35:69–78. [PubMed: 18922643]
13. Forbes GB, Welle SL. Lean body mass in obesity. *Int J Obes* 1983;7:99–107. [PubMed: 6862762]
14. de Divitiis O, Fazio S, Petitto M, Maddalena G, Contaldo F, Mancini M. Obesity and cardiac function. *Circulation* 1981;64:477–82. [PubMed: 7261280]
15. Yoshinari K, Takagi S, Yoshimasa T, Sugatani J, Miwa M. Hepatic CYP3A expression is attenuated in obese mice fed a high-fat diet. *Pharm Res* 2006;23:1188–200. [PubMed: 16715367]
16. Cindik N, Baskin E, Agras PI, Kinik ST, Turan M, Saatci U. Effect of obesity on inflammatory markers and renal functions. *Acta Paediatr* 2005;94:1732–7. [PubMed: 16421032]
17. Salazar DE, Corcoran GB. Predicting creatinine clearance and renal drug clearance in obese patients from estimated fat-free body mass. *Am J Med* 1988;84:1053–60. [PubMed: 3376975]
18. Cheymol G. Effects of obesity on pharmacokinetics implications for drug therapy. *Clin Pharmacokinet* 2000;39:215–31. [PubMed: 11020136]
19. Gidding CE, Kellie SJ, Kamps WA, de Graaf SS. Vincristine revisited. *Crit Rev Oncol Hematol* 1999;29:267–87. [PubMed: 10226730]
20. Moore A, Pinkerton R. Vincristine: Can its therapeutic index be enhanced? *Pediatr Blood Cancer* 2009;53:1180–7. [PubMed: 19588521]
21. Kaspers GJ, Veerman AJ, Pieters R, Van Zantwijk CH, Smets LA, van Wering ER, et al. In vitro cellular drug resistance and prognosis in newly diagnosed childhood acute lymphoblastic leukemia. *Blood* 1997;90:2723–9. [PubMed: 9326239]
22. Lock RB, Liem N, Farnsworth ML, Milross CG, Xue C, Tajbakhsh M, et al. The nonobese diabetic/severe combined immunodeficient (NOD/SCID) mouse model of childhood acute lymphoblastic leukemia reveals intrinsic differences in biologic characteristics at diagnosis and relapse. *Blood* 2002;99:4100–8. [PubMed: 12010813]
23. Behan JW, Yun JP, Proektor MP, Ehsanipour EA, Arutyunyan A, Moses AS, et al. Adipocytes impair leukemia treatment in mice. *Cancer Res* 2009;69:7867–74. [PubMed: 19773440]
24. Lonnerholm G, Frost BM, Abrahamsson J, Behrendtz M, Castor A, Forestier E, et al. Vincristine pharmacokinetics is related to clinical outcome in children with standard risk acute lymphoblastic leukemia. *Br J Haematol* 2008;142:616–21. [PubMed: 18537965]
25. Frost BM, Lonnerholm G, Koopmans P, Abrahamsson J, Behrendtz M, Castor A, et al. Vincristine in childhood leukaemia: no pharmacokinetic rationale for dose reduction in adolescents. *Acta Paediatr* 2003;92:551–7. [PubMed: 12839283]
26. Groninger E, Meeuwssen-de BT, Koopmans P, Uges D, Sluiter W, Veerman A, et al. Pharmacokinetics of vincristine monotherapy in childhood acute lymphoblastic leukemia. *Pediatr Res* 2002;52:113–8. [PubMed: 12084857]
27. Lee JI, Skolnik JM, Barrett JS, Adamson PC. A sensitive and selective liquid chromatography-tandem mass spectrometry method for the simultaneous quantification of actinomycin-D and vincristine in children with cancer. *J Mass Spectrom* 2007;42:761–70. [PubMed: 17511020]
28. Dennison JB, Jones DR, Renbarger JL, Hall SD. Effect of CYP3A5 expression on vincristine metabolism with human liver microsomes. *J Pharmacol Exp Ther* 2007;321:553–63. [PubMed: 17272675]
29. Hartman A, van Schaik RH, van dH I, Broekhuis MJ, Meier M, den Boer ML, et al. Polymorphisms in genes involved in vincristine pharmacokinetics or pharmacodynamics are not related to impaired motor performance in children with leukemia. *Leuk Res*. 2009

30. Renbarger JL, McCammack KC, Rouse CE, Hall SD. Effect of race on vincristine-associated neurotoxicity in pediatric acute lymphoblastic leukemia patients. *Pediatr Blood Cancer* 2008;50:769–71. [PubMed: 18085684]
31. Skolnik JM, Barrett JS, Shi H, Adamson PC. A liquid chromatography-tandem mass spectrometry method for the simultaneous quantification of actinomycin-D and vincristine in children with cancer. *Cancer Chemother Pharmacol* 2006;57:458–64. [PubMed: 16187113]
32. Periclou AP, Avramis VI. NONMEM population pharmacokinetic studies of cytosine arabinoside after high-dose and after loading bolus followed by continuous infusion of the drug in pediatric patients with leukemias. *Cancer Chemother Pharmacol* 1996;39:42–50. [PubMed: 8995498]
33. Avramis VI, Sencer S, Periclou AP, Sather H, Bostrom BC, Cohen LJ, et al. A randomized comparison of native *Escherichia coli* asparaginase and polyethylene glycol conjugated asparaginase for treatment of children with newly diagnosed standard-risk acute lymphoblastic leukemia: a Children's Cancer Group study. *Blood* 2002;99:1986–94. [PubMed: 11877270]
34. Castle MC, Margileth DA, Oliverio VT. Distribution and Excretion of [3H]Vincristine in the Rat and the Dog. *Cancer Res* 1976;36:3684–9. [PubMed: 953993]
35. Junping W, Takayama K, Nagai T, Maitani Y. Pharmacokinetics and antitumor effects of vincristine carried by microemulsions composed of PEG-lipid, oleic acid, vitamin E and cholesterol. *Int J Pharm* 2003;251:13–21. [PubMed: 12527171]
36. Rahmani R, Gueritte F, Martin M, Just S, Cano JP, Barbet J. Comparative pharmacokinetics of antitumor Vinca alkaloids: intravenous bolus injections of navelbine and related alkaloids to cancer patients and rats. *Cancer Chemother Pharmacol* 1986;16:223–8. [PubMed: 3698163]
37. Bender RA, Castle MC, Margileth DA, Oliverio VT. The pharmacokinetics of [3H]-vincristine in man. *Clin Pharmacol Ther* 1977;22:430–5. [PubMed: 902455]
38. Gidding CE, Meeuwssen-de Boer GJ, Koopmans P, Uges DR, Kamps WA, de Graaf SS. Vincristine pharmacokinetics after repetitive dosing in children. *Cancer Chemother Pharmacol* 1999;44:203–9. [PubMed: 10453721]
39. Nelson RL, Dyke RW, Root MA. Comparative pharmacokinetics of vindesine, vincristine and vinblastine in patients with cancer. *Cancer Treat Rev* 1980;7(Suppl 1):17–24. [PubMed: 7438117]
40. Owellen RJ, Root MA, Hains FO. Pharmacokinetics of vindesine and vincristine in humans. *Cancer Res* 1977;37:2603–7. [PubMed: 872088]
41. Cheng Q, Aleksunes LM, Manautou JE, Cherrington NJ, Scheffer GL, Yamasaki H, et al. Drug-metabolizing enzyme and transporter expression in a mouse model of diabetes and obesity. *Mol Pharm* 2008;5:77–91. [PubMed: 18189363]
42. Jackson DV Jr, Bender RA. Cytotoxic Thresholds of Vincristine in a Murine and a Human Leukemia Cell Line in Vitro. *Cancer Res* 1979;39:4346–9. [PubMed: 291476]
43. Anderson SR, Gilge DA, Steiber AL, Previs SF. Diet-induced obesity alters protein synthesis: tissue-specific effects in fasted versus fed mice. *Metabolism* 2008;57:347–54. [PubMed: 18249206]
44. Jackson DV Jr, Nichols AP, Bender RA. Interaction of albumin and vincristine with a human lymphoblastic leukemia cell line in vitro. *Cancer Biochem Biophys* 1980;4:133–6. [PubMed: 6934024]
45. Benet LZ, Hoener BA. Changes in plasma protein binding have little clinical relevance. *Clin Pharmacol Ther* 2002;71:115–21. [PubMed: 11907485]

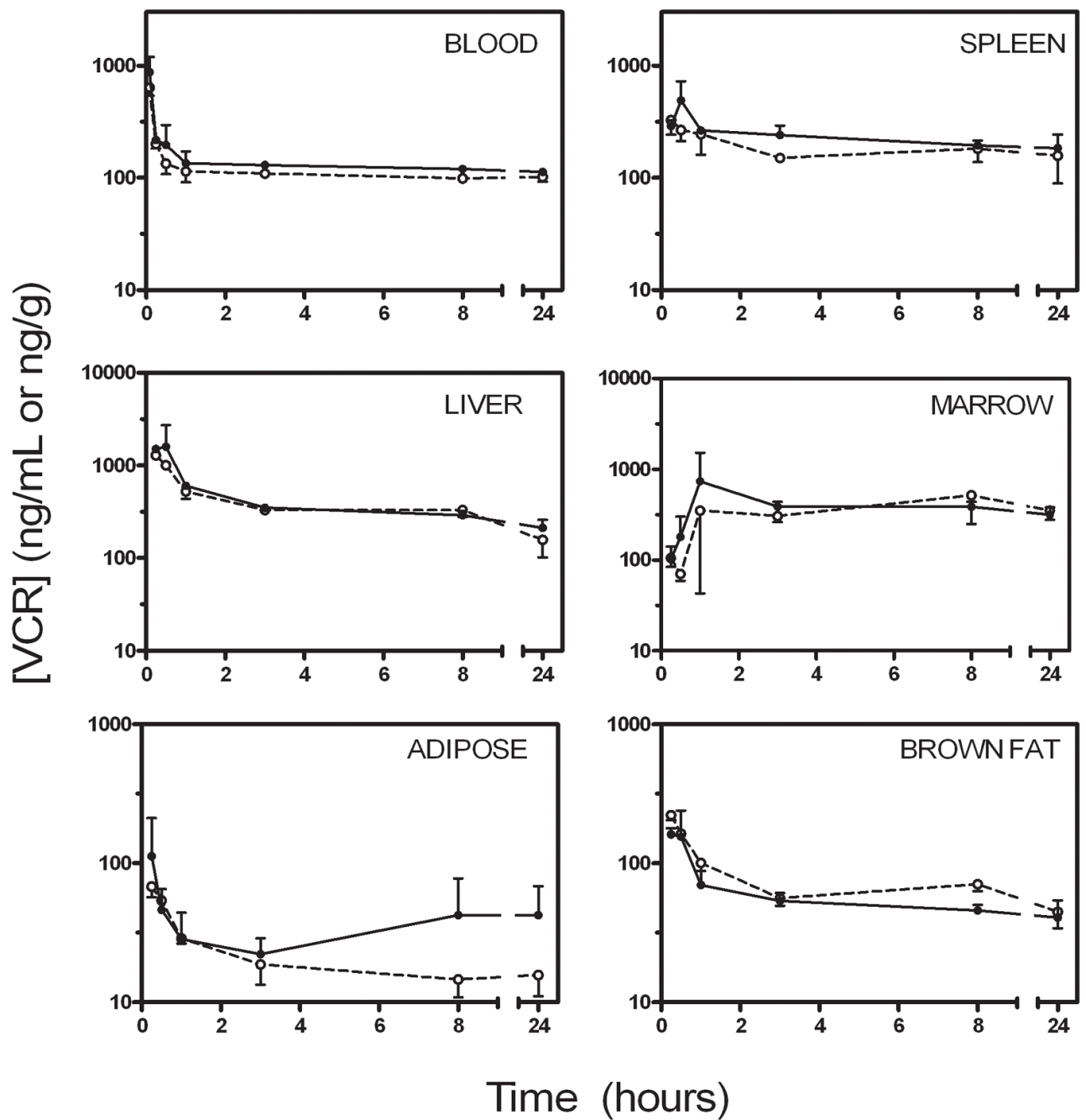


**Figure 1.**

Blood and tissue VCR levels. VCR concentrations in obese (black circles, solid line) and non-obese (open circles, dashed line) mice. VCR concentration is expressed in ng/mL for blood, and ng/gram of wet tissue for all other tissues. (This figure was previously published as a supplementary figure in Behan et al., reference [22])

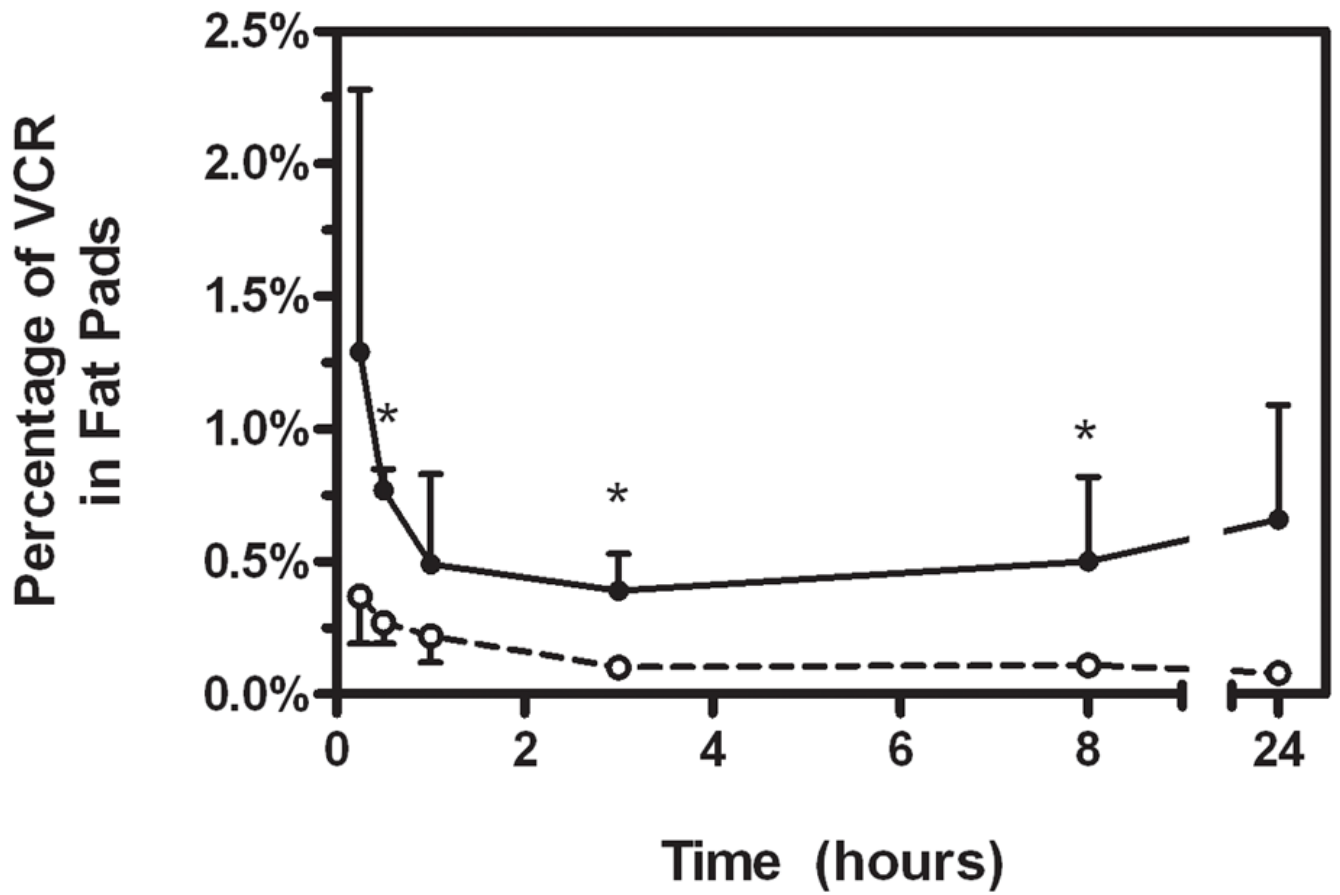


**Figure 2.** Percentage of the injected VCR dose that could be accounted for in the fat pads. Obese (black circles, solid line) and non-obese (open circles, dashed line) mice.

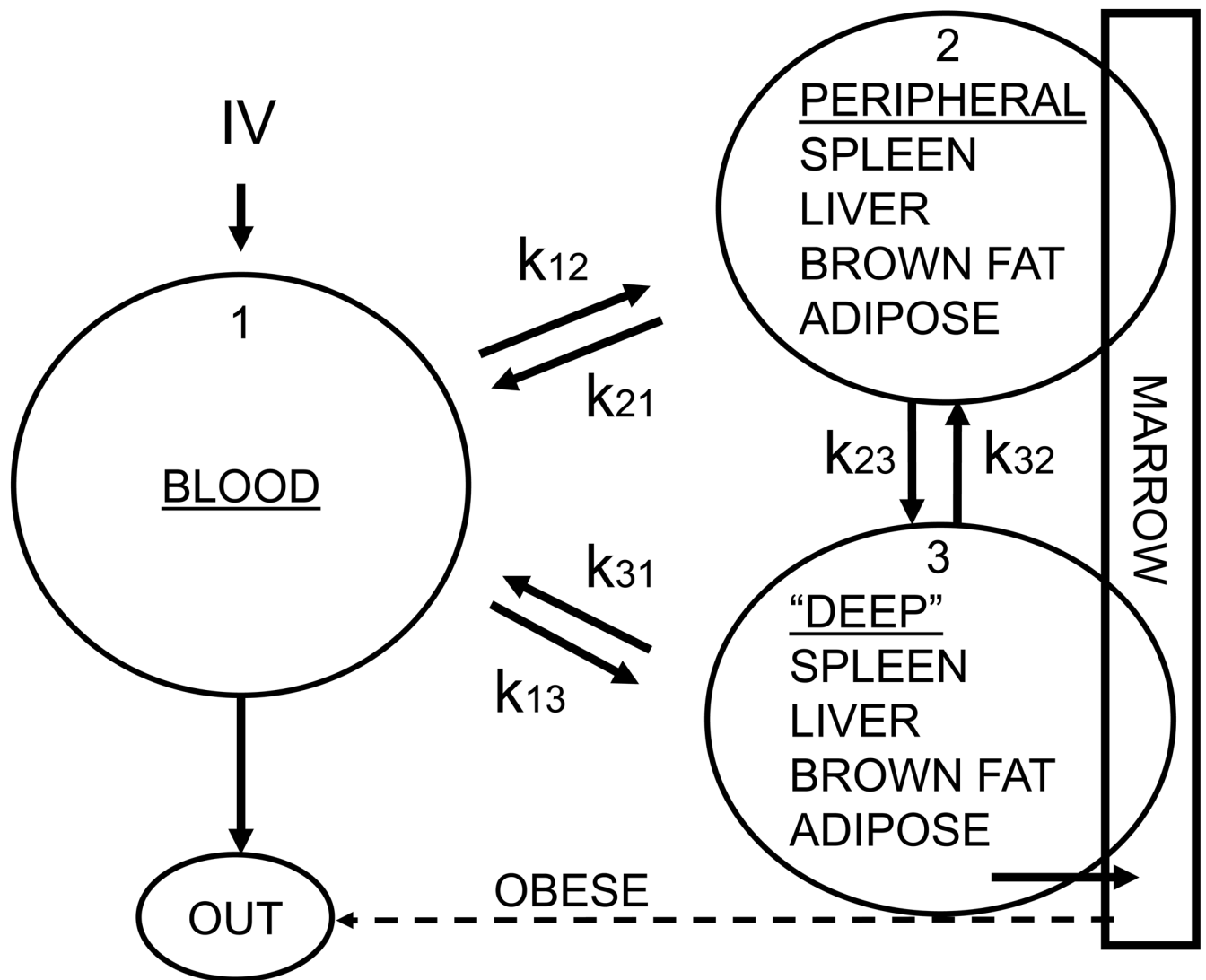


**Figure 3.** Limited physiological PK model of VCR in blood and tissues of lean and obese mice. Dashed arrow illustrates elimination of VCR from the bone marrow of obese mice, which was not apparent in the non-obese mice.

**Table 1**

Non-compartmental analysis results for VCR in blood

	Non-obese	Obese
Dose ( $\mu\text{g}/\text{mouse}$ )	14.7 $\pm$ 0.8	19.7 $\pm$ 2.2
Peak VCR (ng/mL)	2,101	6,331
$t_{1/2,\alpha}$ (min)	4.0	3.5
$t_{1/2,\beta}$ (min)	44.5	9.7
$t_{1/2,\gamma}$ (hrs)	85.6	60.3
AUC <sub>0-24</sub> (ng/mL * hr)	2,846	3,329
AUC <sub>0-<math>\infty</math></sub> (ng/mL * hr)	15,384	13,099
V <sub>DC</sub> (ml/g)	0.238	0.079
V <sub>DSS</sub> (ml/g)	3.81	3.16

**Table 2**

Non-compartmental analysis results for VCR in tissues

	Non-obese		Obese	
	$t_{1/2\beta}$ (min)	$t_{1/2\gamma}$ (hrs)	$t_{1/2\beta}$ (min)	$t_{1/2\gamma}$ (hrs)
Spleen	25.4	43.9	11.9	49.5
Liver	36.7	22.1	23.7	30.5
Bone Marrow	36.2	22.6 <sup>a</sup>	50.7	27.5
Brown Adipose	6.7	18.3	12.4	12.7
White Adipose	16.2	39.2	6.0	56.8

<sup>a</sup> the terminal half-life of VCR in the bone marrow of non-obese mice represents an accumulation—all other half-lives are decay